AFCRC Technical Report 53-13 E5095

A POINT SOURCE BINORMAL LENS WITH WIDE-ANGLE FOCAL POINTS

ELLEN FINE *

and

GEORGE E. REYNOLDS

MAY 1953

ANTENNA LABORATORY

ELECTRONICS RESEARCH DIRECTORATE

AIR FORCE CAMBRIDGE RESEARCH CENTER

CAMBRIDGE, MASSACHUSETTS

* Now with Raytheon Manufacturing Company, Newton, Massachusetts

ABSTRACT

As an extension to the study reported in a previous publication entitled *A Point Source Binormal Lens*, a smaller lens of the same general design, but with focal points spaced farther apart, has been constructed and given similar tests. Field patterns of this X-band model have been made, in addition to the plotting of experimental and theoretical phase-error contours. The geometry of the lens is completely defined by general equations for this type of design.

The overall performance of the lens closely paralleled that of its predecessor, but with improved gain for off-axis positions and decreased coma-lobe level with vertical polarization.

CONTENTS

ILLUSTRATIONS

A POINT SOURCE BINORMAL LENS WITH WIDE-ANGLE FOCAL POINTS *

1. INTRODUCTION

A "binormal" or "constrained" type of lens for use with a point source has been reported in a previous publication.[1] To continue this study, a second point source binormal lens, called the "circlet lens" to distinguish it from the first, has been constructed, also of square tubing, and given similar tests. The circlet lens is the subject of this report.

The inner face of the original lens was a portion of a prolate ellipsoid of revolution with focal points at the foci of the ellipse. The outer face was stepped by integral numbers of wavelengths. Unlike its predecessor, the circlet lens has not been stepped. Both inner and outer faces are continuous portions of ellipsoids.

An application under consideration was the scanning of a wide vertical sector between extreme angles of 32° each side of the axis. This would be accomplished by feeding the lens with an assembly of four horns spaced 16° apart and oscillating ± 8°, as shown in Fig. 1.

In the original lens, the correction points were chosen on lines forming angles of ± 7-1/2° with the axis of the lens. It had been expected that by choosing correction points farther out from the axis, better off-axis behavior would be achieved. When comparison of patterns was made, however, no significant decrease in the side lobes was manifest except for the contribution from the *H*-plane coma lobes for feed positions beyond 10° off-axis.

As mentioned in the previous report, the index of refraction of the lens medium is determined by the spacing between the metal walls parallel to the electric vector. This index is given by

$$n = \sqrt{1 - (\lambda / 2a)^2}\ , \qquad (1)$$

where a is the plate spacing and λ is the free-space wavelength of the electromagnetic wave propagated through the lens. Plans for the circlet lens specified construction from square tubing of 0.700 in. inside diameter and field tests at a wavelength of 2.963 cm. Thus the index of refraction was fixed at 0.55.

---

*Manuscript received for publication August 1952; revised manuscript received 19 January 1953.

[1] W. Ellis, E. Fine, and G. Reynolds (March 1951), "A Point Source Binormal Lens," Rept. No. E5067, AF Cambridge Research Center, Cambridge, Mass.

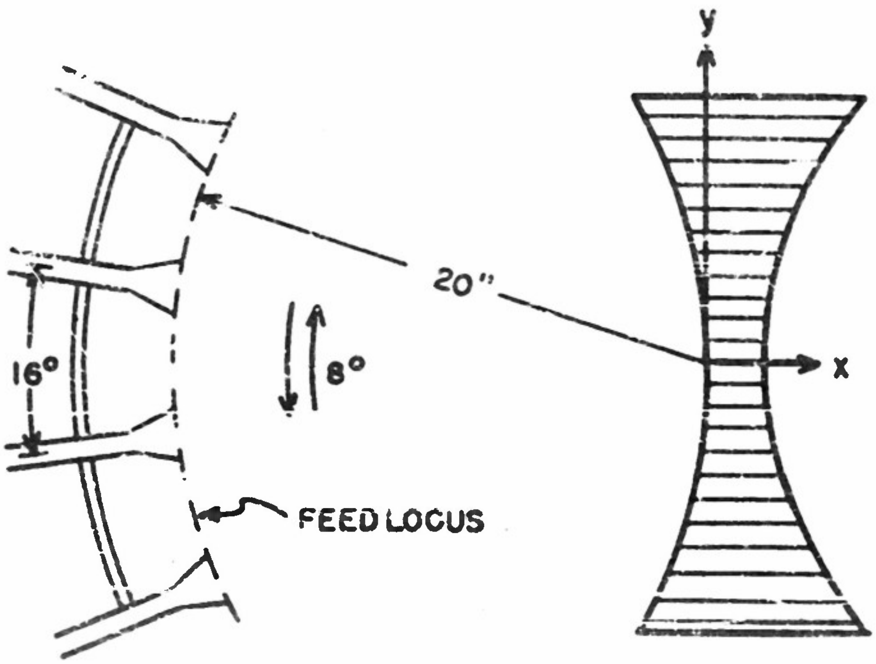

Fig. 1. Oscillating horn feed assembly.

2. DESIGN EQUATIONS

The equations for the design of a lens to focus a plane wave upon a pair of symmetrically positioned points have been derived in the previous report. The equation for the inner face, an ellipsoid of revolution, is given by

$$\left[\frac{x + f\cos\alpha}{f\cos\alpha}\right]^2 + \left[\frac{y}{f}\right]^2 + \left[\frac{z}{f\cos\alpha}\right]^2 = 1\ . \qquad (2)$$

The y, z coordinates of any square tube are defined as those of its axis. Its termination in the inner face is determined by x, and in the outer face by x'. Its length is d. Any point on the outer face, therefore, is designated by (x', y, z) where

$$x' = x + d \quad \text{and} \quad d = d_0 - \frac{x\cos\alpha}{\cos\alpha - n}\ . \qquad (3)$$

The chosen values and definitions of the parameters are:

d_c = 2 in—the thickness of the lens at the center (0,0,0);

f = 20 in.—the distance from the feed source to the center;

α = 22° —the angle measured in the xy-plane between the x-axis and the line joining a focal point to the origin (also the angle of the emanating plane wave when the lens is fed from the correction points).

At one time prior to construction of the lens, it seemed that the required square tubing would not be available and a cardboard model was fabricated in order to study egg-crate construction. Although it was ultimately decided that a tubular lens would be superior to one of egg-crate design, the analysis of the shape of the cardboard sections[2] revealed that the outer surface of the lens was also an ellipsoid, but not one of revolution. Thus, the intersection of the outer surface with any plane normal to a coordinate axis would be an arc of an ellipse.

In the upper portion of Fig. 2 is an example of a planar cut parallel to the xy-plane. The minor axes of the ellipses for the inner face are parallel to the x-axis; for the outer face, it is the major axes that are parallel to the x-axis.

The lower portion of Fig. 2 shows a typical planar cut parallel to the xz-plane. For the inner face this is a circle, and for the outer face an ellipse with major axis parallel to the x-axis as before.

In normalized form the equations for the inner face are:

$$\frac{(x + f \cos \alpha)^2}{f^2 \cos^2 \lambda - z^2} + \frac{y^2}{f^2 - z^2/\cos^2 \alpha} = 1 \tag{4}$$

with z as a parameter and

$$(x + f \cos \alpha)^2 + z^2 = (f^2 - y^2) \cos^2 \alpha \tag{5}$$

with y as a parameter. Inasmuch as circular templates for forming the lens are more easily fabricated than elliptical ones, the latter equation was the one used in dimensioning the templates.

For the outer face the normalized form is

$$\frac{[x' - d_0 + nf \cos \alpha/(n - \cos \alpha)]^2}{n^2 (f^2 \cos^2 \alpha - z^2)/(n - \cos \alpha)^2} + \frac{y^2}{f^2 - z^2/\cos^2 \alpha} = 1 \tag{6}$$

with z as a parameter and

$$\frac{[x' - d_0 + (nf \cos \alpha)/(n - \cos \alpha)]^2}{n^2 (f^2 - y^2) \cos^2 \alpha/(n - \cos \alpha)^2} + \frac{z^2}{(f^2 - y^2) \cos^2 \alpha} = 1 \tag{7}$$

with y as a parameter.

Note that the center of the ellipsoid for the inner face is at the point $(-f \cos \alpha, 0, 0)$ and for the outer face at $[d_0 - nf \cos \alpha/(n - \cos \alpha), 0, 0]$.

---

[2]The task of scribing ellipses on the cardboard sections led to the construction of a trammel ellipsograph. The ellipses in Fig. 2 were drawn to scale upon the instrument designed by T. T. Pureka, now with the Instrumentation Lab. at Mass. Inst. Tech.

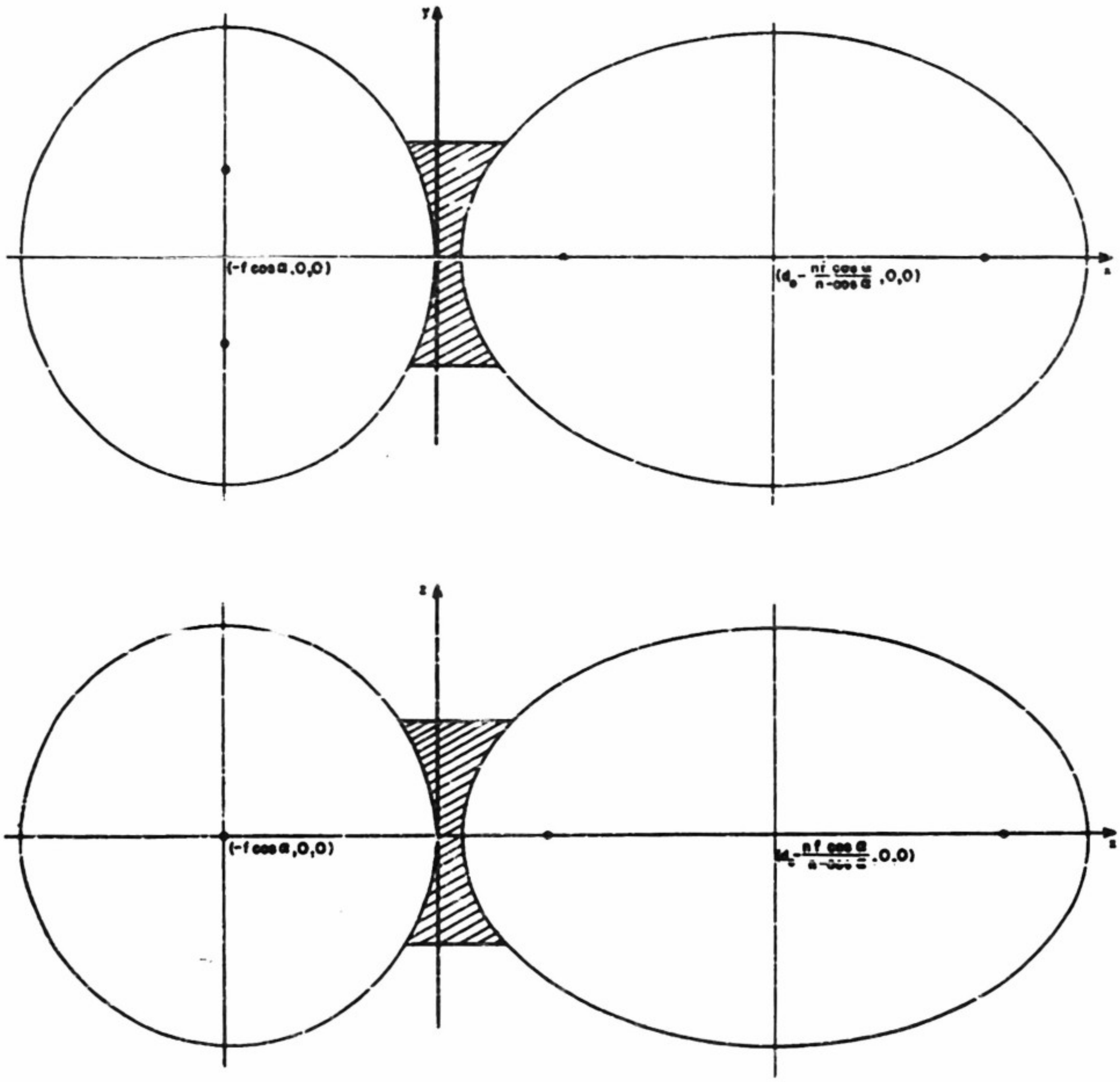

Fig. 2. Ellipsoidal cross sections.

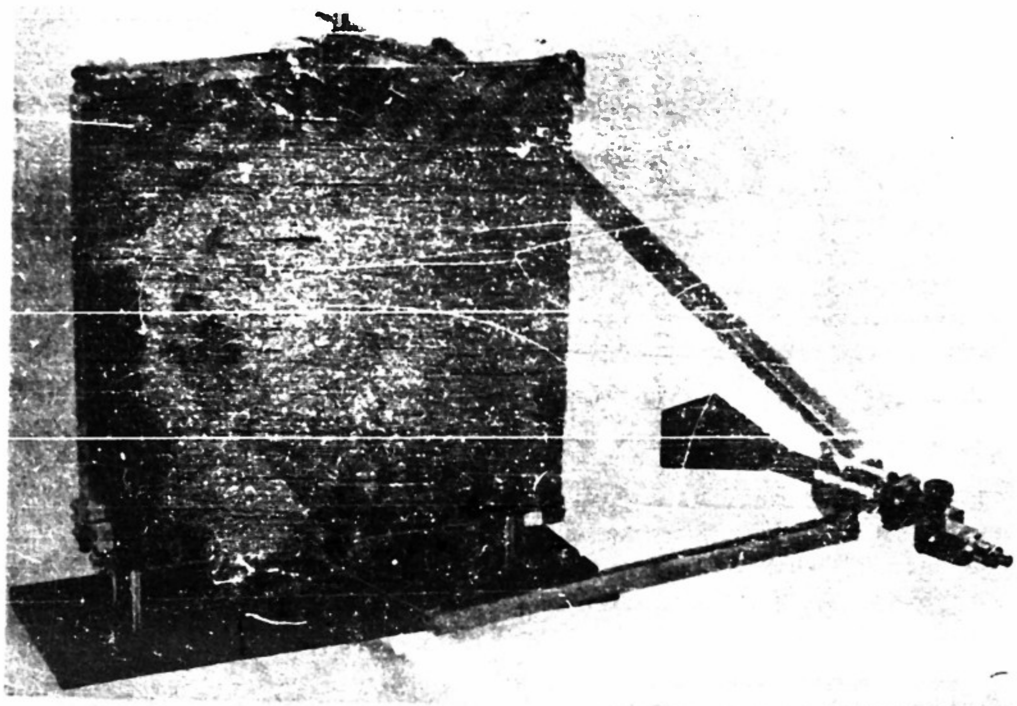

(a)

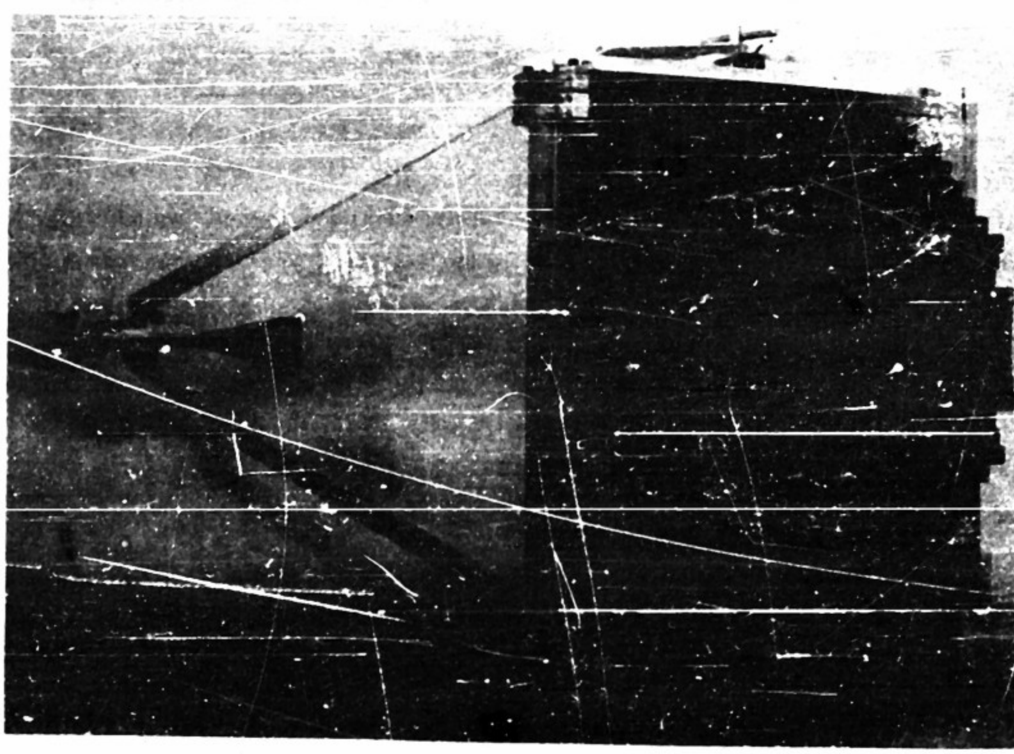

(b)

Fig. 3. Inner and outer faces of the circlet lens. (a) Inner face (b) Outer face.

3. EXPERIMENTAL MODEL

The photographs in Fig. 3 show that the periphery of the lens is roughly circular, with a radius of 18-1/2 tube widths to give an f/d ratio of one.

To obtain the lengths of the tubes and their relative positions, Eq. (2) was solved for x and then evaluated, together with d, on punched card machinery. Because of the symmetrical design, it was necessary to figure only one quadrant.

The lens was constructed from 561 lengths of square tubing of 0.700 in. ± 0.002 in. i.d. and 0.010 in. ± 0.002 in. wall thickness. Each length of this thin-walled tubing was cut upon a lathe after the insertion of a mandril, which was cut simultaneously. Since for economy of mandrils, it was desirable to start cutting with the longest and continue in descending order of length, the tube lengths were arranged in this order by the punched card machinery.

As before, each row was formed by butting the individual tubes against a template and soldering each tube to the one adjacent. Then the rows were stacked against the templates (assembled in an array) and soldered. A square Textolite frame and spacers were employed to hold the entire assembly together.[3]

4. FIELD PATTERNS

All test patterns[4] were made at the design wavelength of 2.963 cm at the Ipswich test station. The feed used for this lens, like the one used for its predecessor, was a rectangular horn flared to produce an illumination approximately 10 db down from peak power at the edges of the lens in both the electric and the magnetic planes.

Examination of the initial patterns revealed that reflections from the V-shaped feed holder had contributed to the level of the side lobes. This necessitated the retaking of a few patterns after a different type of feed holder had been constructed.

A set of patterns was taken for comparison of the circlet lens with the preceding point source binormal lens to learn whether a significant change in the off-axis focusing characteristics had been effected by the 22° correction points. These comparisons are shown in the plots of Fig. 4, where the peak power of each lens on axis has been normalized to zero.

The lens was mounted with its xy-plane horizontal. Azimuth patterns were taken with the horn at various positions along the feed locus shown in Fig. 1. With the polarization vertical, the best focus was

---

[3] The technique of assembly and assiduous construction of the circlet lens are the work of N. O. Hansen and W. J. Kearns of the Antenna Lab., Electronics Research Directorate, AF Cambridge Research Center.

[4] For most of the data obtained, acknowledgment is made to C. R. Forbes who, with the assistance of H. J. Henkel, took more than 300 patterns.

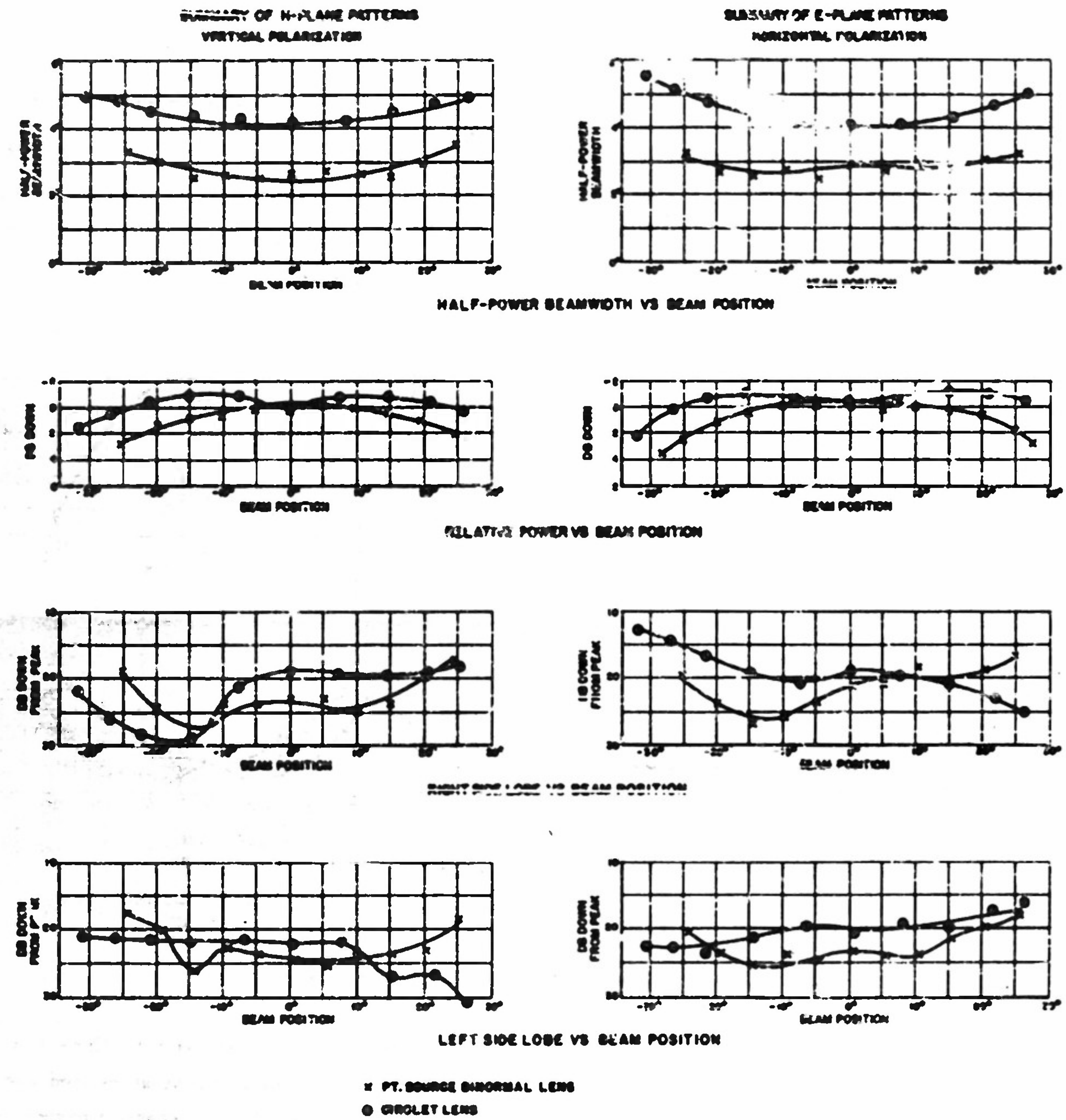

Fig. 4. Graphs for comparison of the circlet lens with its predecessor.

found with the mouth of the horn adjusted to 18-1/2 in. from the center of the lens, measured along its axis. For the horizontal polarization, the best focus was found at 19-3/4 in.

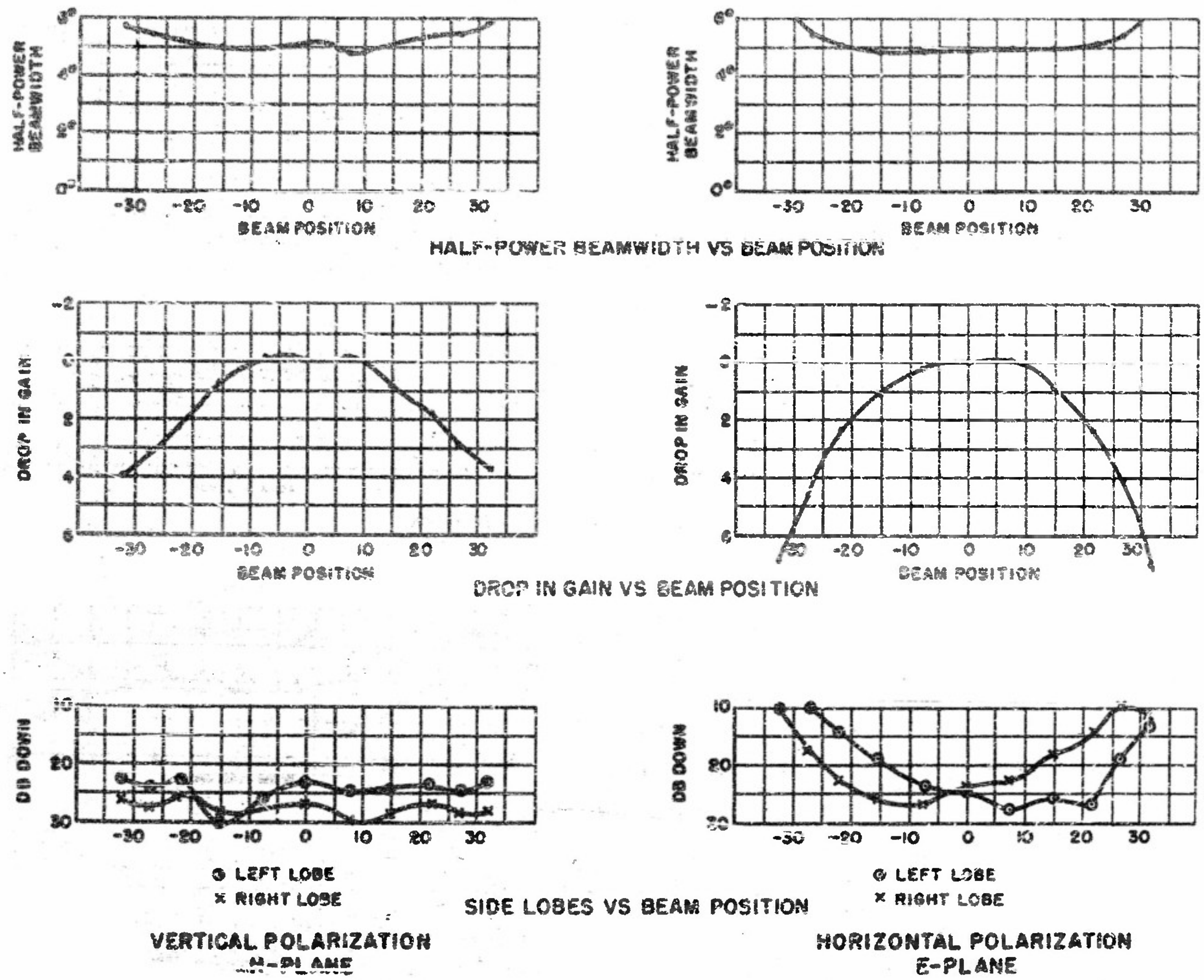

Fig. 5. Data from azimuth patterns with elliptical plane vertical.

The expected increase in half-power beamwidths due to the decreased aperture was evident. There was improvement in the relative power in that the gain did not fall off but even increased at first as the feed was moved off-axis. The gain was greater near the correction points than it was on-axis. For negative angles of off-axis feed positions, the right side lobe is the coma lobe and for positive angles it is the left lobe. In the *H*-plane patterns the coma lobes of the circlet lens in patterns beyond 10° are lower than those of the point source binormal lens, even though they are somewhat higher on-axis. In the E-plane patterns, this coma lobe suppression is not manifest.

For a second set of patterns the lens was rotated 90° on its own axis so that the *xy*-plane became vertical. Azimuth patterns were taken as before. The feed was focused on-axis at 14-1/2 in. from the lens center for vertical polarization and at 16 in. for the horizontal.

The graphs of the results are plotted in Fig. 5. They are seen to be somewhat more symmetrical than the corresponding curves of Fig. 4. The beamwidth is somewhat greater, but the relative power has dropped off. The side lobes average out about the same.

5. PHASE STUDY

When the circlet lens is fed from the correction points — i.e., at the angle α and from a distance f — theoretically there is no phase error. If the feed is moved along an arc of constant radius f through an angle θ, which is measured in the same manner as α (see Fig. 6), then the phase error δ at a particular point is defined as the difference between the electrical path length through the center and that through the point. This is given by

$$\delta = \sqrt{(x + f\cos\theta)^2 + (y + f\sin\theta)^2 + z^2} - f - y\sin\theta + nx(\cos\alpha - \cos\theta)/(n - \cos\alpha) \,. \qquad (8)$$

A point of nearly maximum phase error is the point upon the periphery of the lens where $y = 0$ and z is a maximum. The value of α was chosen by comparing the path lengths through this point from the two extreme positions along the feed circle, i.e., where $\theta = 0°$ and $\theta = 32°$. When α is fixed at 22°, the phase errors are numerically equivalent, though opposite in sign.

Fig. 6. Sketch of path length differences.

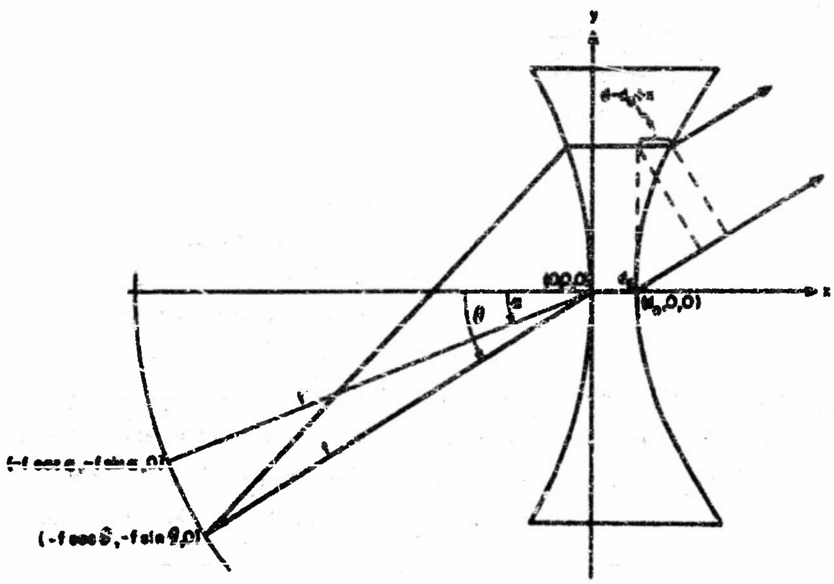

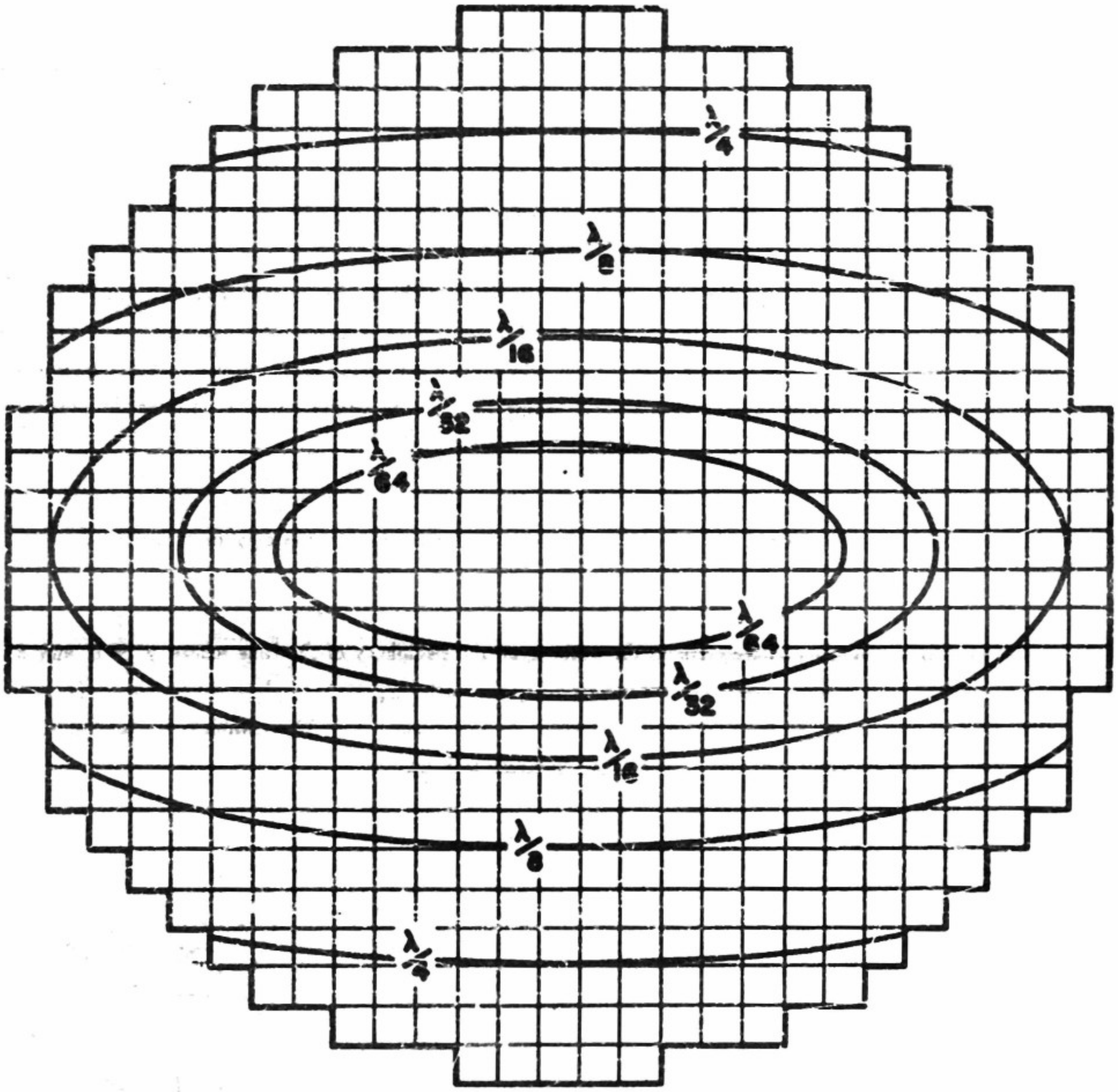

Fig. 7. Phase error contours for feed on axis.

Equation (8) was evaluated with θ fixed at zero for each tube in one quadrant, and also with θ fixed at 32° for each tube in two quadrants. Because of symmetry this data was sufficient to provide the contours over the entire face of the lens which are depicted in Figs. 7 and 8.

All values of δ were divided by λ so that the data could be plotted in terms of the wavelength. The

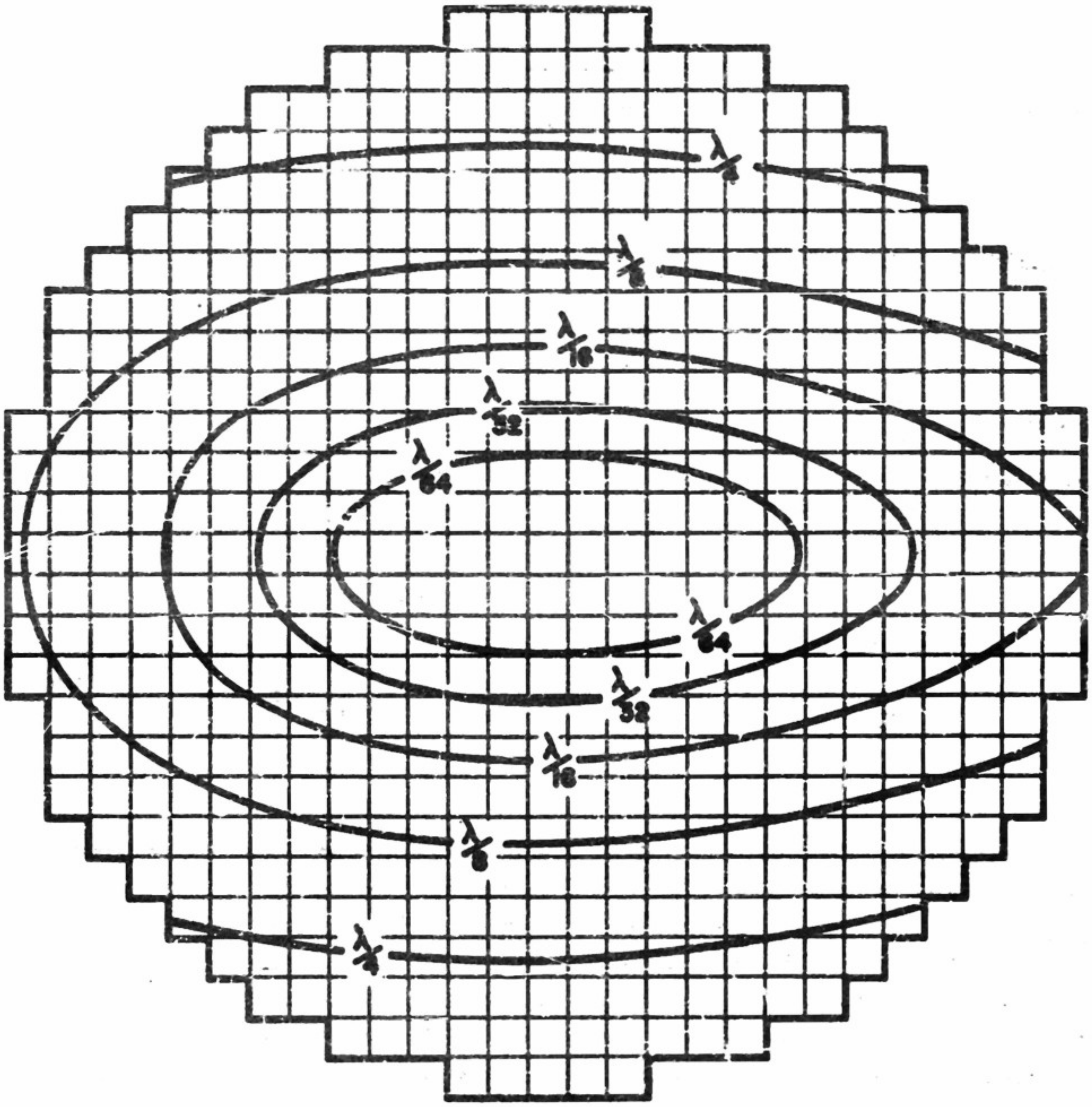

Fig. 8. Phase error contours with feed at 32°.

layout of squares in these figures is representative of the actual tubes in the lens. Figure 7 shows the phase errors when $\theta = 0°$, while Fig. 8 is the error plot for $\theta = 32°$.

A second locus for the feed was considered, i.e., along the circle passing through the two correction points and the origin. The two feed circles are diagramed in Fig. 9. Equation (8) was modified to take into account the new geometric positions with phase error defined by δ_c;

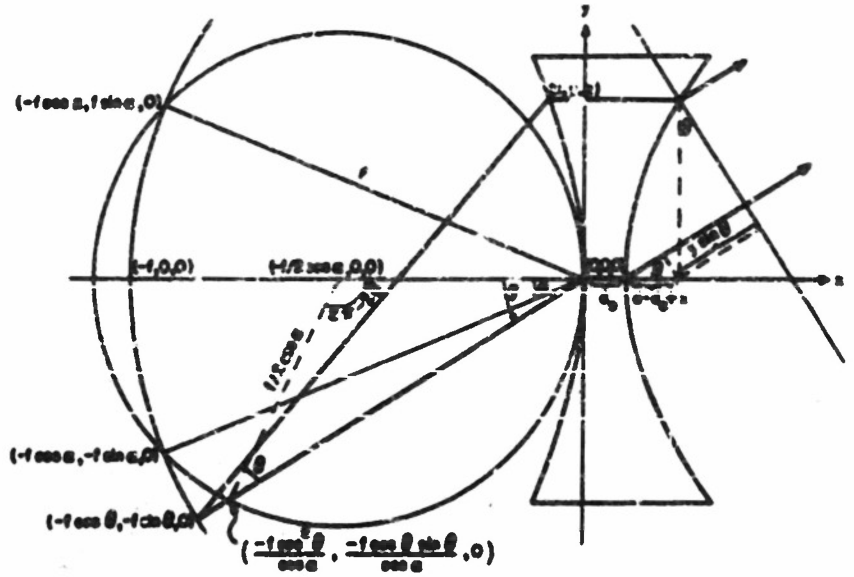

Fig. 9. Feed circle through correction points and origin.

$$\delta_e = \sqrt{\left(x + \frac{f\cos^2\theta}{\cos\alpha}\right)^2 + \left(y + \frac{f\sin\theta\cos\theta}{\cos\alpha}\right)^2 + z^2} + nd - \left[\frac{f\cos\theta}{\cos\alpha} + nd_0 + (d - d_0 + x)\cos\theta + y\sin\theta\right] . \quad (9)$$

After rearrangement and simplification by utilizing the square-root series in lieu of the radical, this equation was solved many times to obtain the points necessary for plotting the additional contours shown in Figs. 10 and 11. These, also, are in terms of the wavelength and are superimposed for comparison purposes upon the contours of Figs. 7 and 8, respectively.

A study of these figures quickly reveals that the error is increased at all points, because each contour of the modified position of the feed (light line) is entirely enclosed by the contour of the same phase error for the design position (heavy line). Indeed, an error of 1/2 wavelength can be found near the edge of the lens.

Actual measurements of the phase errors were made on the automatic phase plotter[5] in the Airborne Section of the Antenna Laboratory. No means were available for taking measurements within a plane parallel to the face of the lens as would be desirable. Instead, plots were made in planes perpendicular,

[5] R. M. Barrett and M. H. Barnes (Jan. 1952), "Automatic Antenna Wave-Front Plotter," *Electronics* 25, No. 1, beginning p. 120.

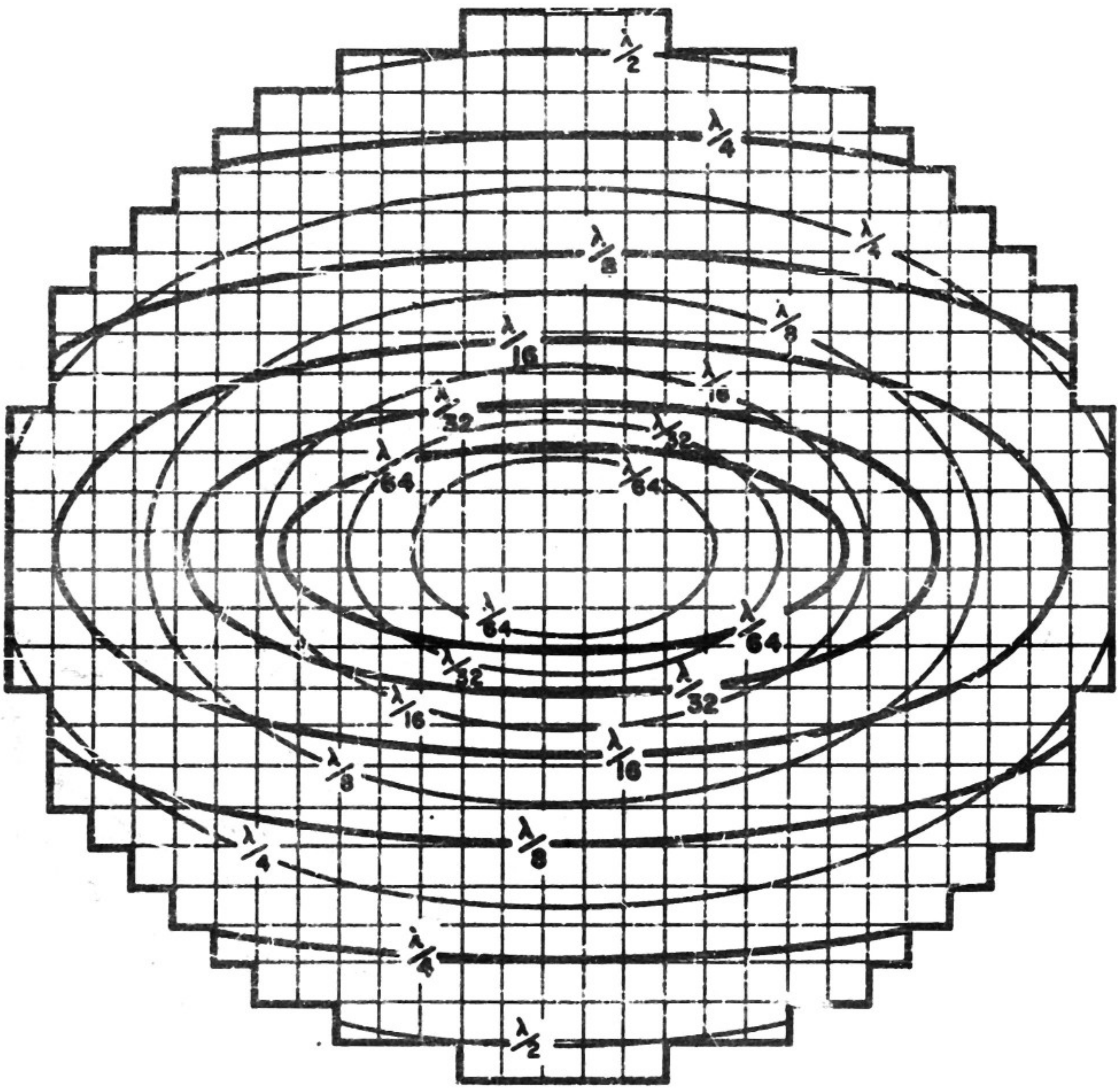

Fig. 10. Error contours from modified feed circle for feed on axis.

i.e., in the xy-plane or the xz-plane. Three different feed angles were used: 0°, 22° and 32°. Sample sections of these plots are shown in Fig. 12. All were made at a wavelength of 3.12 cm, the closest approach that could be made to the design wavelength of 2.963 cm with the equipment on hand.

The straight phase fronts are visual evidence of the collimating ability of the lens.

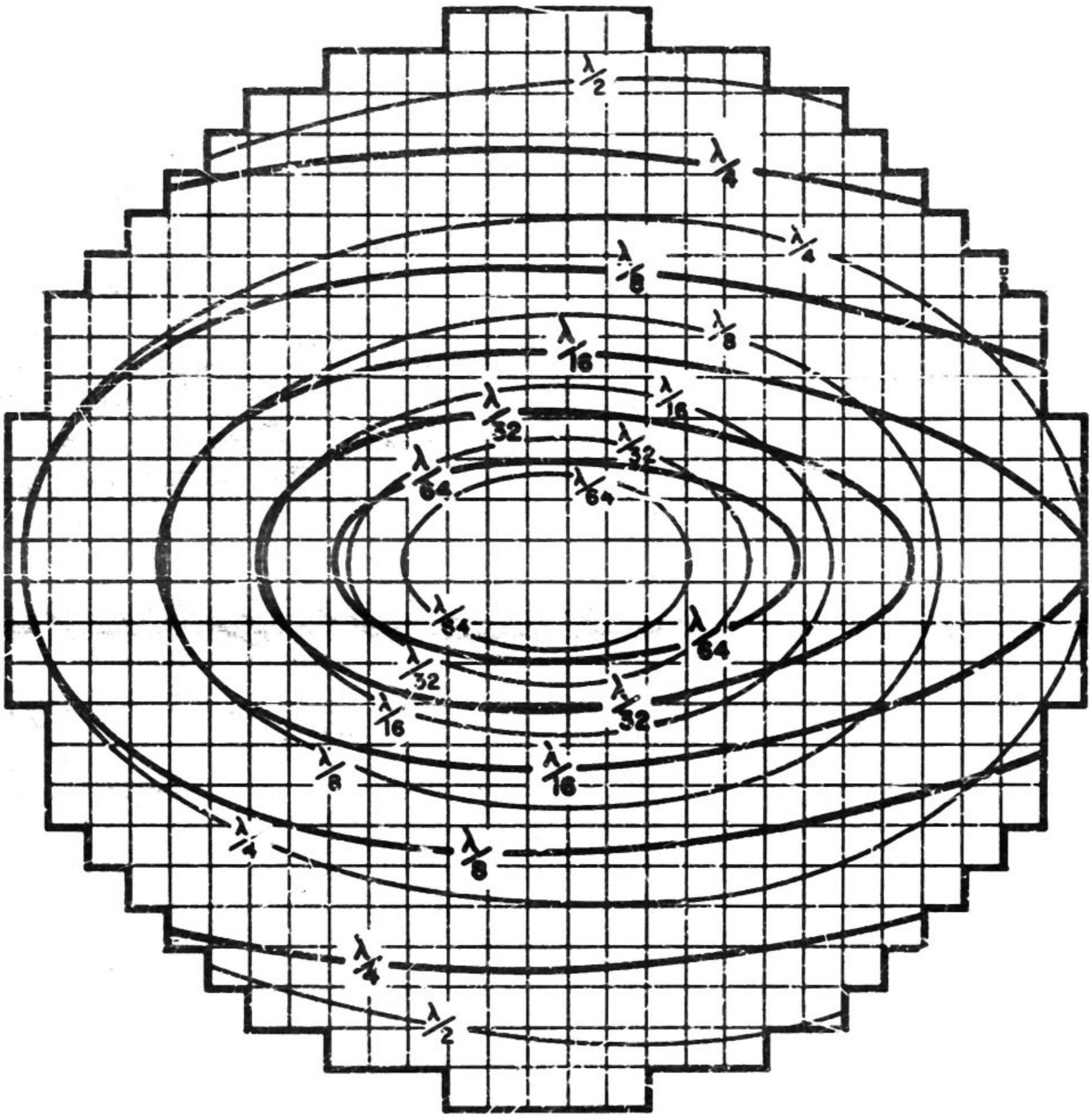

Fig. 11. Error contours from modified feed circle with feed at 32°.

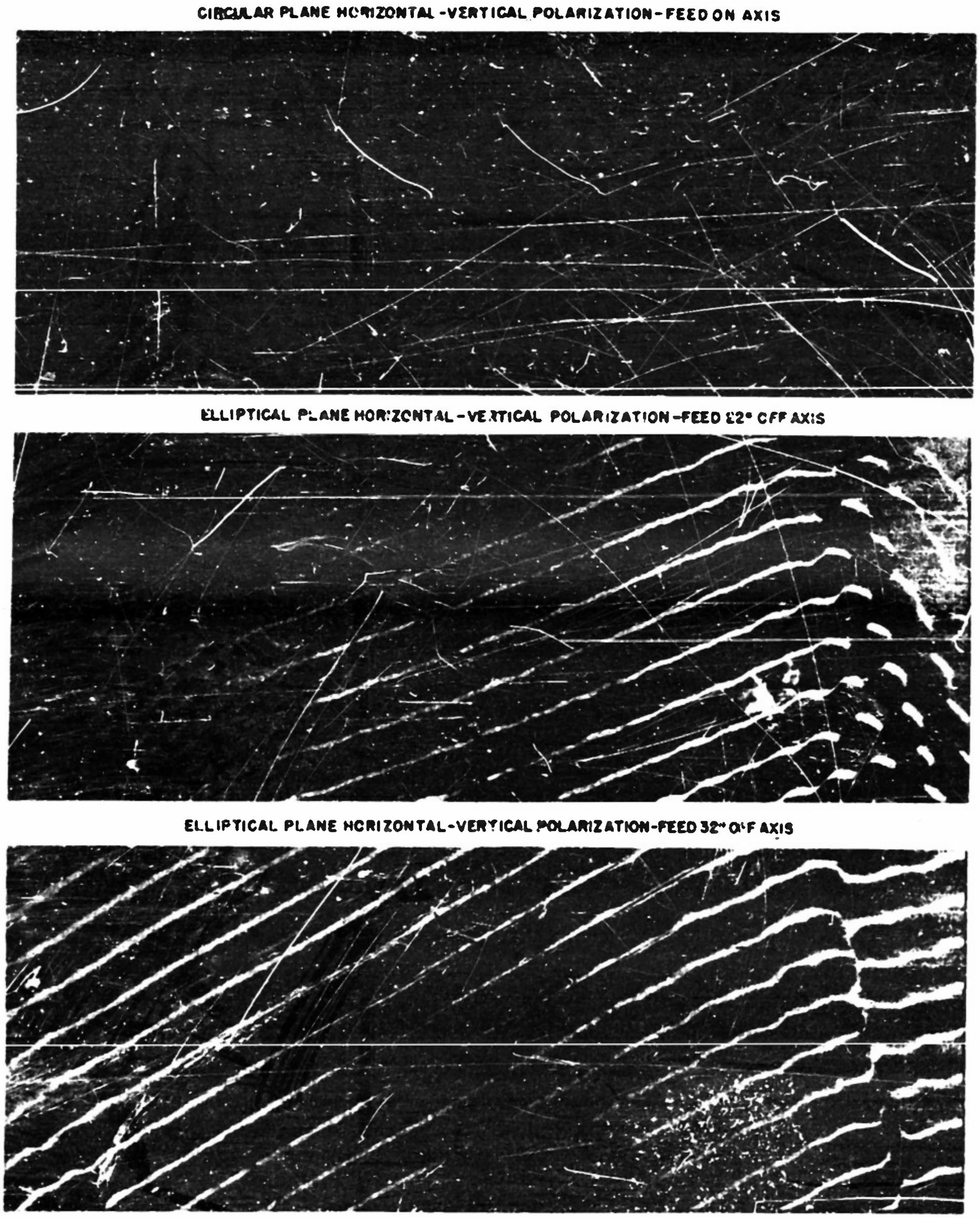

Fig. 12. Automatic phase plots.

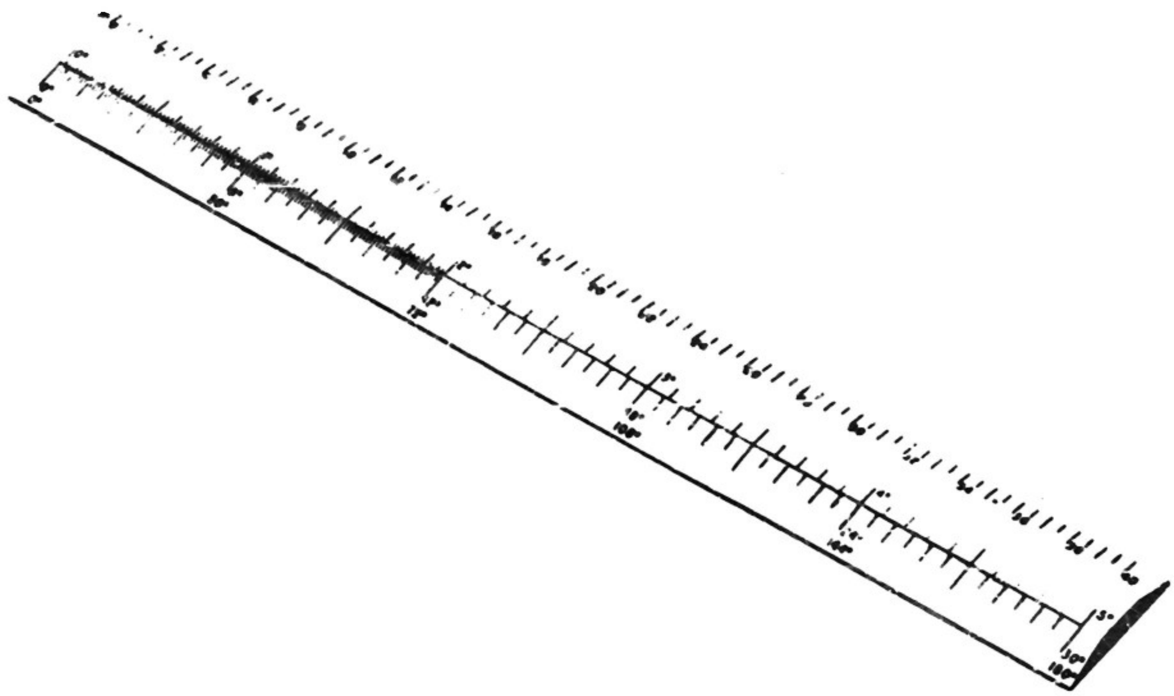

Fig. 13. Pattern scale.

6. APPENDIX

The need to glean data from a large number of patterns obtained with the circlet lens led to the pattern reading device illustrated in Fig. 13. The reader may wish to design a similar tool adapted to his own pattern paper.

The scale is made from transparent plastic, beveled to the edges. The engravings are on the under side and are filled in red to set them off from the black grid lines of the pattern paper.

The scale at the edge is graduated in decibels for measuring the depth of side lobes below the peak and for measuring relative levels of peaks.

The other scale has a line running through its center, with three sets of graduations whose major marks align with those of the pattern paper. Only one set is used at a time, depending on the ratio of paper travel to antenna rotation at which the recorder is operated. The location of this line is at a critical distance (3.01 db) below the top edge previously mentioned. Thus, the half-power beamwidth may be read quickly by placing the top edge tangent to the peak of the pattern and indexing the zero upon the left slope. The reading is taken at the intersection of the right slope with the line.